



Drought counteracts soil warming more strongly in the subsoil than in the topsoil according to a vertical microbial SOC model

Marleen Pallandt^{1,2}, Marion Schrumpf¹, Holger Lange³, Markus Reichstein¹, Lin Yu⁴ and Bernhard Ahrens¹

- 5 1. Max Planck Institute for Biogeochemistry, Jena, Germany
2. International Max Planck Research School (IMPRS) for Global Biogeochemical Cycles, Jena, Germany
3. Norwegian Institute of Bioeconomy Research, Ås, Norway
4. Department of Earth System Sciences, Hamburg University, Hamburg

Correspondence to: Marleen Pallandt (marleen.pallandt@natgeo.su.se)

10 **Abstract.** Soil organic carbon (SOC) is the largest terrestrial carbon pool, but it is still uncertain how it will respond to climate change. Especially the fate of SOC due to concurrent changes in soil temperature and moisture is uncertain. It is generally accepted that microbially driven SOC decomposition will increase with warming, provided that sufficient soil moisture, and hence enough C substrate, is available for microbial decomposition. We use a mechanistic, microbially explicit SOC decomposition model, the Jena Soil Model (JSM), and focus on the depolymerisation of litter and microbial residues by
15 microbes at different soil depths, and its sensitivities to soil warming and different drought intensities. In a series of model experiments we test the effects of soil warming and droughts on SOC stocks, in combination with different temperature sensitivities (Q_{10} values) for the half-saturation constant K_m ($Q_{10,Km}$) associated with the breakdown of litter or microbial residues. Microbial depolymerisation rates of litter and residues are proportional to microbial biomass (reverse kinetics), so that at low microbial biomass, the temperature sensitivity of K_m plays a more prominent role. We find that soil warming leads
20 to long-term SOC losses, but depending on SOC composition and its associated $Q_{10,Km}$ values, these losses can be either reduced or further accelerated, especially in the subsoil where microbial biomass is low. Droughts can alleviate the effects of soil warming and reduce SOC losses, and even lead to SOC gains, provided unchanged litter inputs. Furthermore, a combination of drought and different $Q_{10,Km}$ values associated with the breakdown of litter or microbial residues can have counteracting effects on the overall decomposition rates. In this study, we show that while absolute SOC changes driven by
25 soil warming and drought are highest in the topsoil, SOC in the subsoil is more sensitive to the (sometimes counteracting) interplay between K_m , temperature and soil moisture changes, and mineral-associated SOC.

1 Introduction

Soils are an important component of the global carbon (C) cycle as they store large quantities of C. Soils can act as C sources or sinks, depending on the balance between C inputs and outputs over time. Apart from plant litter inputs, microbial residues
30 are recognised as important precursors for the formation of stable, mineral-associated soil organic carbon (Cotrufo et al., 2013; Liang et al., 2017; Xiao et al., 2023). Therefore, to determine whether soils are a net C source or sink, the speed at which soil organisms decompose litter inputs and existing soil organic carbon (SOC) stocks including microbial residues is of particular importance (Kallenbach et al., 2016). Soil temperature and soil moisture are the two most important controlling factors of microbial decomposition rates, and thereby the carbon turnover rate of soils (Davidson and Janssens, 2006; Moyano et al.,
35 2013; Yan et al., 2018). The interaction between microbial SOC decomposition and (de)stabilisation of SOC to mineral surfaces is another important factor determining the fate of SOC stocks (Ahrens et al., 2020; Dwivedi et al., 2017; Sokol et al., 2022). As SOC decomposition and its future variations depend on soil properties as well as climate, understanding and



representing the complex feedbacks between climate change and SOC decomposition in models is extremely important for future climate projections.

40 Microbes process SOC by depolymerizing a wide array of C substrates such as plant litter and microbial residues that greatly differ in their chemistry (Buckeridge et al., 2022; Cotrufo and Lavallee, 2022). In models, the microbial depolymerisation rate can be described using reverse Michaelis-Menten (MM) kinetics (Tang and Riley, 2019), where a maximum depolymerisation rate (V_{max}) is multiplied with a MM-term that describes the diffusion of extracellular enzymes to a C substrate. A simple formulation of the MM-term is depicted in conceptual Fig. 1 with the term $C_B/(K_m + C_B)$, where C_B is the microbial biomass and K_m is the half-saturation constant for the reaction. Both V_{max} and K_m are temperature sensitive, where V_{max} increases with
45 higher temperatures. The temperature sensitivity of K_m , however, has been shown to be negative or positive depending on which enzymes are involved in the breakdown of C substrates: Allison et al. (2018b) reported $Q_{10,Vmax}$ values between 1.48 - 2.24, and $Q_{10,Km}$ values between 0.7 - 2.8., where a value below denotes a negative temperature sensitivity. $Q_{10,Km}$ can modify K_m by the relationship:

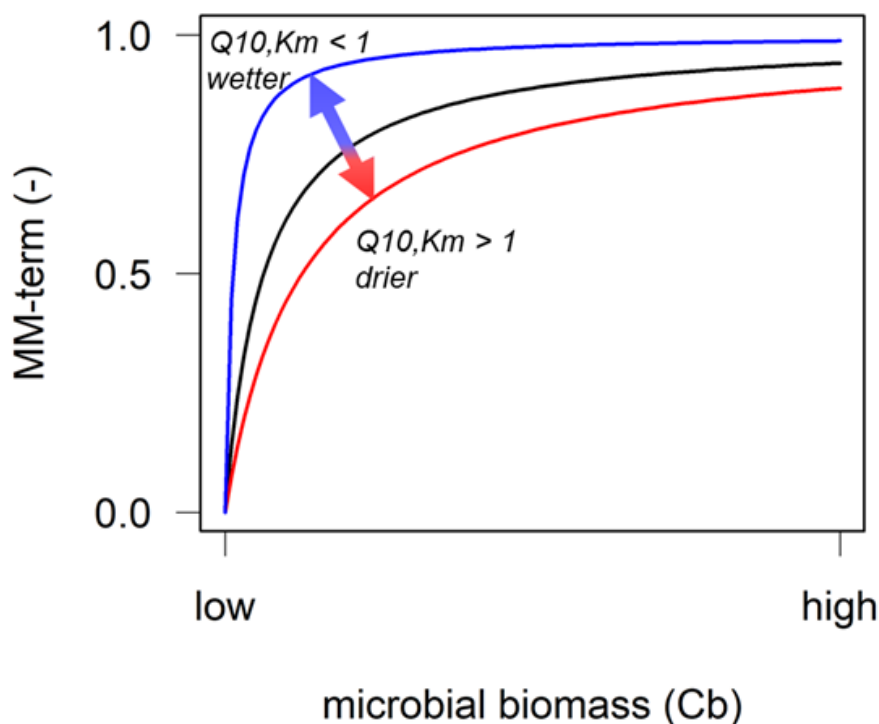
$$50 \quad K_m = K_{m,ref} \times Q_{10,Km}^{(T - T_{ref})/10} \quad (1)$$

Where T and T_{ref} are the soil temperature and a reference temperature, respectively. The MM-term also depends on soil moisture, where lower soil moisture values result in stronger microbial limitation on enzymatic depolymerisation (Zhang et al., 2022).

$$K_m = K_{m,ref} \times \left(\frac{\theta}{\theta_{fc}}\right)^{-3} \quad (2)$$

55 Where θ and θ_{fc} are volumetric soil moisture and volumetric soil moisture at field capacity, respectively. Additionally, high soil moisture values result in lower oxygen availability - which can be described by a second MM-term (Skopp et al., 1990; Davidson et al., 2012). Global mean soil warming is expected to be $4.5 \text{ °C} \pm 1.1 \text{ °C}$ by the end of this century (Soong et al., 2020), but for projected soil moisture changes there is much more uncertainty. While in mediterranean climates and desert ecosystems temperature and soil moisture may be inversely correlated (e.g. García-García et al., 2023; Zhang et al., 2020),
60 projected global lateral and vertical distributions of future soil moisture are more diverse (Berg et al., 2017) and highly depend on anthropogenic greenhouse gas and aerosol emissions (Wang et al., 2022b).

The effect of soil moisture on substrate availability, and thus on the MM kinetics under a warming climate, depends on the value of $Q_{10,Km}$. This interplay between different $Q_{10,Km}$ values and soil moisture has the potential to lead to counteracting effects on the overall decomposition rates, where the short-term responses on heterotrophic respiration have been shown in modelling studies (Davidson et al., 2006; Davidson and Janssens, 2006; Sierra et al., 2015). More specifically, at low microbial
65 biomass and $Q_{10,Km}$ values > 1 , an increase in K_m as a result of warming can ‘compensate’ or counteract the expected increase in SOC decomposition rates through $Q_{10,Vmax}$ (Davidson et al., 2006). These model studies, however, highly simplify the system as they do not consider a dynamic substrate pool, i.e. there is no interaction between the microbial pool (with its own growth and turnover rates) and the in- and outputs of different C substrate pools. To understand changes in SOC stocks on
70 longer time scales, however, the microbial dynamics have to be included as well.



75 **Figure 1:** Conceptual depiction of the relationship between microbial biomass (C_B) and the Michaelis-Menten (MM) term $C_B/(K_m + C_B)$ to represent microbial limitation of depolymerisation. Soil moisture & temperature effects on half-saturation constant K_m can increase or decrease the MM-term through Eqs. 1 and 2. The black line shows the MM-term when $Q_{10, K_m} = 1$ and soil moisture is unchanged. The MM-term decreases when the soil gets drier or when $Q_{10, K_m} > 1$ (red line), and increases when the soil gets wetter or $Q_{10, K_m} < 1$ (blue line).

80 Besides the inclusion of microbial dynamics, it is important to consider soil moisture and temperature changes along a vertical gradient (Pallandt et al., 2022), because projected soil moisture may not change in the same direction for surface and deeper soil layers (Fig. 2 in Berg et al., 2017). As SOC, microbial biomass and mineral-associated SOC are also not distributed evenly within soil profiles, the interactions between soil moisture, microbes and substrates will vary with depth. This requires a model which includes vertically resolved, mechanistic descriptions of microbially driven decomposition and organo-mineral interactions so that C substrate depletion by microbes or sorption can be explicitly simulated. However, the vast majority of SOC decomposition models integrated in coupled climate models are highly empirical and have very simple process representation using first-order decomposition rates adopted from the CENTURY approach (Parton et al., 1987). Recent insights have led to the development of SOC decomposition models which take into account microbial (enzymatic) processes and sometimes organo-mineral interactions (e.g. Abramoff et al., 2017; Sulman et al., 2014; Wieder et al., 2014; Zhang et al., 2022). Another limitation of these models as well as the classic ones is that they generally only consider one soil depth (Wieder et al., 2015) and as a result, can fail to capture observed climate sensitivities of soil carbon turnover times (Ahrens et al., 2015; Braakhekke et al., 2011; Koven et al., 2013, 2017; Pallandt et al., 2022).



In this study, we bridge these gaps by applying the C cycle version of the Jena Soil Model (JSM, Yu et al., 2020) to investigate the interplay between microbial depolymerisation and climate change. JSM is a vertically resolved, mechanistic SOC decomposition model. It includes organo-mineral interactions, is microbially explicit, and uses mechanistic descriptions of the various physiological processes affecting microbial SOC decomposition affected by temperature and soil water content, such as substrate and oxygen availability. JSM's modular structure offers the opportunity to study the various soil temperature and soil moisture controls on SOC decomposition either individually or simultaneously. We focus on the following research questions: 1) How do temperature and soil moisture changes affect modelled SOC decomposition through V_{max} and the Michaelis-Menten term?; and 2) Do top- and subsoil layers respond differently to warming and drought? In a series of model experiments we test the effects of soil warming and droughts on SOC stocks, in combination with different $Q_{10,Km}$ values which are associated with the depolymerisation of the polymeric litter pool or of microbial residues.

2 Methods

2.1 Model description

JSM is a vertically explicit soil organic matter (SOM) decomposition model with microbial interactions on SOM decomposition, and representation of organic matter (de)sorption to mineral surfaces. For this study, we represent and describe the C cycle, but JSM is also capable of simulating the coupled C,N and P cycles and isotope (^{13}C , ^{14}C , ^{15}N) tracking. A full mathematical description of JSM and its coupled nutrient cycles can be found in the supplement material of Yu et al. (2020). Here, we summarise the most important C cycle processes relevant to this study, with a conceptual overview in Fig. 2 and parameters and units listed in Table 1.

Above- and belowground non-woody litter inputs are partitioned into soluble and polymeric litter following Parton et al. (1993). JSM does not explicitly simulate enzyme production, but these are implicitly described using Michaelis-Menten (MM) kinetics. For the depolymerisation steps reverse Michaelis-Menten kinetics are used, as Tang and Riley (2019) found these to be more appropriate than traditional, forward MM-kinetics. The depolymerisation of litter or microbial residues to the dissolved organic carbon (DOC) pool is described as:

$$f_{depoly,X} = V_{max,X} \times f_{V_{max,X}}(T_{soil}) \times C_X \times \frac{C_B}{K_{mX} \times f_{K_{mX}}(T_{soil},\theta) + C_B} \quad (3)$$

so that the depolymerisation rate is limited by the size of the microbial biomass pool (C_B). X is either the polymeric litter pool (P) or the microbial residues pool (R), $V_{max,X}$ is the maximum specific depolymerisation rate of X , C_X is the respective litter pool X , and C_B is the microbial biomass pool. $f_{V_{max,X}}(T_{soil})$ is an exponential function expressed with a Q_{10} base (Wang et al., 2012):

$$f_{V_{max,X}}(T_{soil}) = Q_{10,V_{max,X}} \frac{T_{soil} - T_{ref}}{10} \quad (4)$$

where $Q_{10,V_{max,X}}$ is the temperature sensitivity of the maximum specific depolymerisation rate of litter pool X , and T_{soil} and T_{ref} are the soil temperature or reference temperature, respectively.

125

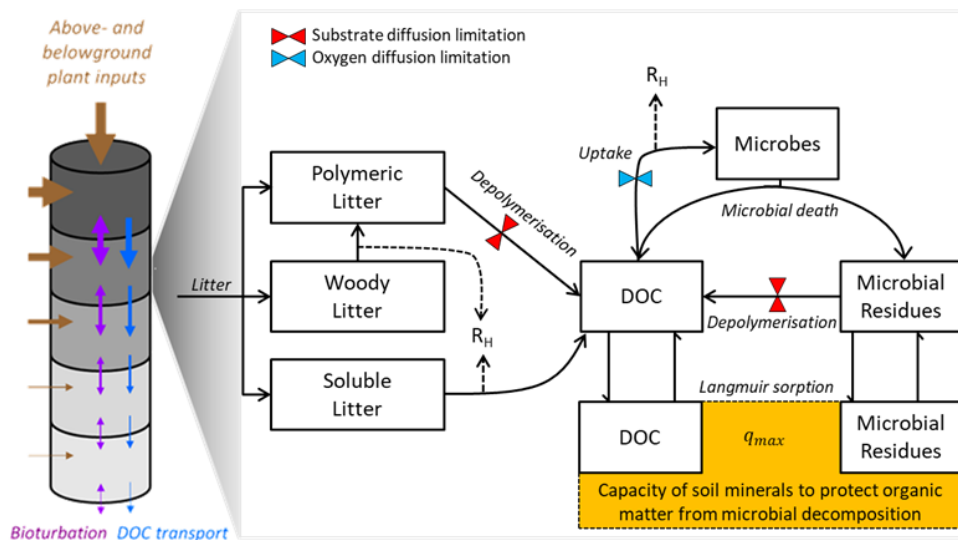


Figure 2: Schematic representation of the C cycle in JSM, after Yu et al. (2020), showing C pools (rectangles) and C fluxes (line arrows) between pools. DOC: Dissolved Organic Carbon, q_{max} : maximum sorption capacity for sorption of DOC and microbial residues to mineral surfaces. The dotted lines are heterotrophic respiration (R_H) fluxes. The coloured hourglasses represent different soil moisture controls on SOC decomposition steps: microbial limitation of depolymerisation (red), and oxygen limitation (blue) on microbial uptake.

130

Table 1: Parameter values related to temperature sensitive processes in JSM.

Parameter	Value	Unit	Reference
$V_{max,P}$	0.1849	yr ⁻¹	Yu et al. 2020
$V_{max,R}$	0.2317	yr-1	Yu et al. 2020
$V_{max,U}$	95.76	day-1	Yu et al. 2020
$K_{m,P}$ and $K_{m,R}$	3.70	mmol C m-3	Yu et al. 2020
$K_{m,U}$	85.26	mol C m-3	Yu et al. 2020
$Q_{10,Vmax,U}$	1.98		Allison et al. (2010)
$Q_{10,Vmax,P}$ and $Q_{10,Vmax,R}$	2.16		Wang et al. (2012)
$Q_{10,Km,P}$	1.31*		Allison et al. (2018b)
$Q_{10,Km,R}$	0.7*		Allison et al. (2018b)
$Q_{10,adsorption}$	1.08		Wang et al. (2013)
$Q_{10,desorption}$	1.34		Wang et al. (2013)
R	8.314	J K ⁻¹ mol ⁻¹	
T_{ref}	293.15	K	Wang et al. (2012)

135



The Q_{10} coefficient is the ratio of reaction rates when temperature increases by 10 °C. For use within JSM, all Q_{10} values were converted to activation energies (E_a) following Eq. (7) from Wang et al. (2012):

$$Q_{10} = \exp \left[\frac{E_a}{R \times T_{ref}} \times \frac{10}{T_{soil}} \right] \quad (5)$$

where R is the universal gas constant, and T_{soil} and T_{ref} are the soil temperature and reference temperature, respectively.

140 Inclusion of soil moisture is done through Eq. (6):

$$f_{Km,x}(T_{soil}, \theta) = Q_{10,Km,x} \frac{T_{soil} - T_{ref}}{10} \times \left(\frac{\theta}{\theta_{fc}} \right)^{-3} \quad (6)$$

This is a function to describe the sensitivity of the half-saturation constant (Km_x) to soil moisture and temperature, where $Q_{10,Km,x}$ is the temperature sensitivity of the half-saturation constant of C_x , and where θ and θ_{fc} are the volumetric water content and water content at field capacity, respectively.

145 Microbial C uptake for growth is described using traditional, forward MM-kinetics (Tang and Riley, 2019):

$$f_{Uptake} = V_{max,U} \times f_{Vmax,x}(T_{soil}) \times C_B \times \frac{C_{DOC}}{K_{m,U} + C_{DOC}} \times \frac{a^{4/3}}{K_{m,O_2} + a^{4/3}} \quad (7)$$

so that the uptake rate is limited by the size of the available substrate (C_{DOC}) and by the air-filled pore space (a), which is calculated as

$$a = \frac{\theta_{fc} - \theta}{\theta_{fc}} \quad (8)$$

150 and functions as a proxy to describe the amount of oxygen available for the reaction (Davidson et al., 2012). $V_{max,U}$ is the maximum uptake rate of DOC by C_B , C_{DOC} is the dissolved organic C pool, $K_{m,U}$ is the half-saturation constant for the uptake of DOC by C_B and K_{m,O_2} is the half-saturation constant of the reaction with oxygen. DOC and microbial residues can be protected from microbial decomposition by sorption to mineral surfaces (Fig. 2). In JSM, adsorption and desorption rates are temperature sensitive (Q_{10} values reported in Table 1), with a full description of the process implementation in Ahrens et al. (2020). * Q_{10} values are reported for the model's reference temperature (T_{ref}) of 20 °C, and their respective activation energies were calibrated for JSM in an earlier study (Yu et al., 2020), or taken from literature by Ahrens et al. (2020). Values marked with * are unique to this study and taken from Allison et al. (2018b), and measured at a reference temperature of 16 °C. Activation energies for JSM were adjusted accordingly using Eq. (5).

2.2 Modelling protocol

160 The stand-alone application of JSM requires depth-specific soil temperature, soil moisture and litterfall forcing data at a half hourly time step as input. These were generated by running the QUINCY model for 500 years beforehand using meteorological forcing data from 1901 - 1930, and then starting a transient simulation in combination with FLUXNET3 forcing data from 1901 - 2012 as described in Thum et al. (2019), for a temperate forest site in Germany (DE-Hai). These site-specific soil forcing data are then used for model spinup for 500 years, where soil forcing data from 2000 - 2012 are used repeatedly. After
 165 spinup, JSM is run for 100 simulation years for each model experiment (Section 2.4).



2.3 Choice of $Q_{10,Km}$ values for polymeric litter and microbial residues

Microbes process SOC by depolymerizing a wide array of C substrates derived from plant litter or microbial residues, which greatly differ in their chemistry (Buckeridge et al., 2022; Cotrufo and Lavallee, 2022). In JSM, the polymeric litter and microbial residues pool are depolymerised by extracellular enzymes produced by the microbial pool (C_B) to enter the DOC pool (Fig. 2, Eq. (3)). Enzyme production is not explicitly simulated, but assumed to be proportional to the size of the microbial biomass pool. The half-saturation constants for depolymerisation of polymeric litter and microbial residues ($K_{m,X}$, Eq. (3)) are sensitive to temperature, but knowledge about their value is restricted to laboratory studies of individual enzymes. In this study, we explore different temperature sensitivities, expressed as Q_{10} values, for our model's half-saturation constants for microbial depolymerisation of polymeric litter ($K_{m,P}$) and microbial residues ($K_{m,R}$). We base these Q_{10} values on a study from Allison et al. (2018b), who give an extensive overview of the temperature sensitivities of different enzymes and their substrate targets. We chose values from this study that would likely be, or closely resemble, the main enzymes involved in the breakdown of our model's polymeric litter (C_P) and microbial residue (C_R) pools. For the depolymerisation of C_P we targeted a $Q_{10,Km,P}$ value measured for the enzymes β -xylosidase and total oxidase, as these are involved in the degradation of hemicellulose, lignin and phenolics. For the depolymerisation of C_R we selected a $Q_{10,Km,R}$ value measured for the enzyme leucine aminopeptidase, which is involved in the degradation of polypeptides, the main component of microbial cell walls. In the various model experiments (described in more detail in section 2.4), we explore the effects of these different temperature sensitivities on SOC decomposition individually, or combined.

2.4 Model experiments

During the first model run, ambient soil moisture and soil temperature are used repeatedly for a 100-year simulation. We do this to check whether the SOC pools between 0 - 50 cm depth still increase/decrease over the simulation period, i.e. to verify that the SOC pools reached steady state after the 500 year spinup period. Then, to investigate the effects of soil warming on SOC decomposition, we run the first set of soil warming experiments. Soils, including the deep soil up to 1m, are expected to warm by 4.5°C by the end of the century under representative concentration pathway (RCP) 8.5 (Soong et al., 2020), so we increased all ambient soil temperatures by 4.5 K throughout the 100 year simulation period, keeping the original seasonality in the ambient input data intact without altering the ambient soil moisture (SM) values. To test the sensitivity of SOC decomposition to warming and to investigate the potential feedbacks through the temperature sensitivity of the Michaelis-Menten term, we ran each warming experiment using different values for $Q_{10,Km,P}$ and $Q_{10,Km,R}$ (Table 1): Both $Q_{10,Km,P}$ and $Q_{10,Km,R}$ values are 1 (i.e. not temperature sensitive); Individual Q_{10} values for the breakdown of the microbial residue pool and the polymeric litter pool, where $Q_{10,Km,R}$ is set to 0.7 and $Q_{10,Km,P}$ is set to 1.3; Both $Q_{10,Km,P}$ and $Q_{10,Km,R}$ are 0.7 (representing the breakdown of microbial residues); Both $Q_{10,Km,P}$ and $Q_{10,Km,R}$ are 1.3 (representing the breakdown of the litter pool);. All model experiment settings are summarised in Table 2.

Then, to investigate the effects of soil warming and drying on SOC decomposition, we run the first set of drought experiments, where we keep all $Q_{10,Km,X}$ values at 1 and use ambient soil temperature + 4.5 K. Soil drying is expected for most of the globe (Wang et al., 2022b and references therein), but drought intensity is uncertain and may vary locally (Cook et al., 2020; Hsu and Dirmeyer, 2023). Therefore, we compare three simple model drought scenarios, where the model's ambient SM inputs are reduced by 10% : In three model experiments, each ambient SM value is multiplied by 0.9, 0.8 or 0.7, respectively (Table 2). As with the warming experiment, the original seasonality in the ambient SM input values is kept intact.



As a last step, we investigate the combined effects of soil warming and drying on SOC decomposition including the feedback through the half-saturation constants' temperature sensitivities. Similar to the first set of 3 drought experiments, ambient soil temperature is raised by 4.5 K, and three different drought intensities are simulated ($SM * 0.9$, $SM * 0.8$ and $SM * 0.7$). Reflecting the most likely realistic combination of $Q_{10,Km}$ values for microbial depolymerisation, as soil will contain both microbial residues as well as polymeric litter for microbes to depolymerise, we used the two individual Q_{10} values from Allison et al. (2018b) for the breakdown of the microbial residue pool and the polymeric litter pool ($Q_{10,Km,R} = 0.7$ and $Q_{10,Km,P} = 1.3$).

2.5 Model output analyses

Each model experiment was run for 100 simulation years, yielding daily output files for different soil variables. We calculate SOC stocks as the sum of the soluble litter, polymeric litter, DOC, microbial residues, adsorbed DOC and adsorbed microbial residues pools (Fig. 2). Woody litter is excluded as it is considered part of the aboveground litter layer. To calculate the annual changes in SOC stocks, expressed as percentage change (%) since the start of the simulation, we used SOC values from the last day of each simulation year. All analyses and plots were done using packages "tidyverse", "ggplot2" and "viridis" under R version 4.3.1 in Rstudio (Garnier et al., 2023; R Core Team, 2023; RStudio Team, 2018; Wickham, 2016; Wickham et al., 2019).

3 Results

3.1 Warming effects on SOC decomposition

3.1.1 Modelled SOC stock changes at ambient and elevated soil temperatures

To check whether JSM reached steady state after spinup, one model run was continued with ambient soil temperatures and soil moisture, and with $Q_{10,Km,X}$ values of 1 (not temperature sensitive), i.e., the same setup as during spinup. The first 6 soil layers (0 - 50 cm) are in steady state at Hainich forest, as there is no SOC loss or gain over the complete simulation period (Fig. 3, dark blue). The small interannual variability in modelled SOC stocks reflects the interannual variability in the litter inputs and other forcing. Warming the soil by 4.5 K in a model experiment leads to SOC losses for all simulation years (Fig. 3, purple) until 5.1% of initial stocks are lost by the end of the simulation period (Table 2). The topsoil loses more SOC (- 6.2%) than the subsoil (- 3.9%), which is related to the fact that mineral-associated organic C (MAOC) increases with depth which leaves less available substrates for microbes to depolymerise in the subsoil (Fig. A1), as well as the lower microbial biomass in these layers which strongly reduces the Michaelis-Menten term for the depolymerisation rates (Fig. 1). Additionally, the processes of adsorption and desorption have lower temperature sensitivities than microbial processes in JSM so that warming affects the topsoil layers more strongly than the deeper layers where more SOC is mineral-associated. The soil warming effect is strongest at the beginning of the simulation period, but reduces as the model returns to a new steady state after roughly 100 simulation years.



Table 2: Model experiments and settings with simulated changes (%) in SOC stocks at three different depth intervals

Experiment	ST	SM	$Q_{10,Km,R}$	$Q_{10,Km,P}$	Δ SOC (%) 0 - 50 cm	Δ SOC (%) 0 - 6 cm	Δ SOC (%) 36 - 50 cm
1. Ambient model run	+ 0.0 K	SM * 1.0	1	1	0	0	0
2. Warming experiments	+ 4.5 K	SM * 1.0	1	1	-5.1	-6.2	-3.9
	+ 4.5 K	SM * 1.0	0.7	0.7	-6.8	-7.3	-5.6
	+ 4.5 K	SM * 1.0	1.3	1.3	-4.0	-5.5	-2.8
3. Drought experiments	+ 4.5 K	SM * 1.0	0.7	1.3	-5.2	-6.4	-3.9
	+ 4.5 K	SM * 0.9	1	1	-3.0	-4.4	-1.9
	+ 4.5 K	SM * 0.8	1	1	+1.0	-1.1	+1.6
4. Combined experiments	+ 4.5 K	SM * 0.7	1	1	+6.8	+3.8	+7.1
	+ 4.5 K	SM * 0.9	0.7	1.3	-3.1	-4.6	-2.0
	+ 4.5 K	SM * 0.8	0.7	1.3	+0.5	-1.5	+1.2
	+ 4.5 K	SM * 0.7	0.7	1.3	+5.8	+3.1	+6.1

235

3.1.2 Temperature sensitivity of half-saturation constants

To study the effects of temperature on SOC decomposition through the half-saturation constant for depolymerisation ($Q_{10,Km,X}$), the model was run using three different combinations of $Q_{10,Km,X}$ values for the depolymerisation of the polymeric litter and microbial residues pools (Table 2): Both $Q_{10,Km,X}$ are 0.7; both $Q_{10,Km,X}$ are 1.3; or $Q_{10,Km,R}$ is 0.7 and $Q_{10,Km,P}$ is 1.3. Using a Q_{10} value for half-saturation constants $K_{m,P}$ and $K_{m,R}$ of 0.7 (reflecting the temperature sensitivity of the depolymerisation of microbial residues) substantially accelerates SOC losses in response to warming. SOC losses until 50 cm depth reach 6.8% (Fig. 3, pink points). The topsoil loses more SOC than the subsoil (-7.3 % and -5.6 %, respectively), but when comparing with the run that uses $Q_{10,Km,X}$ values of 1 the relative difference in the subsoil is larger than in the topsoil.

240



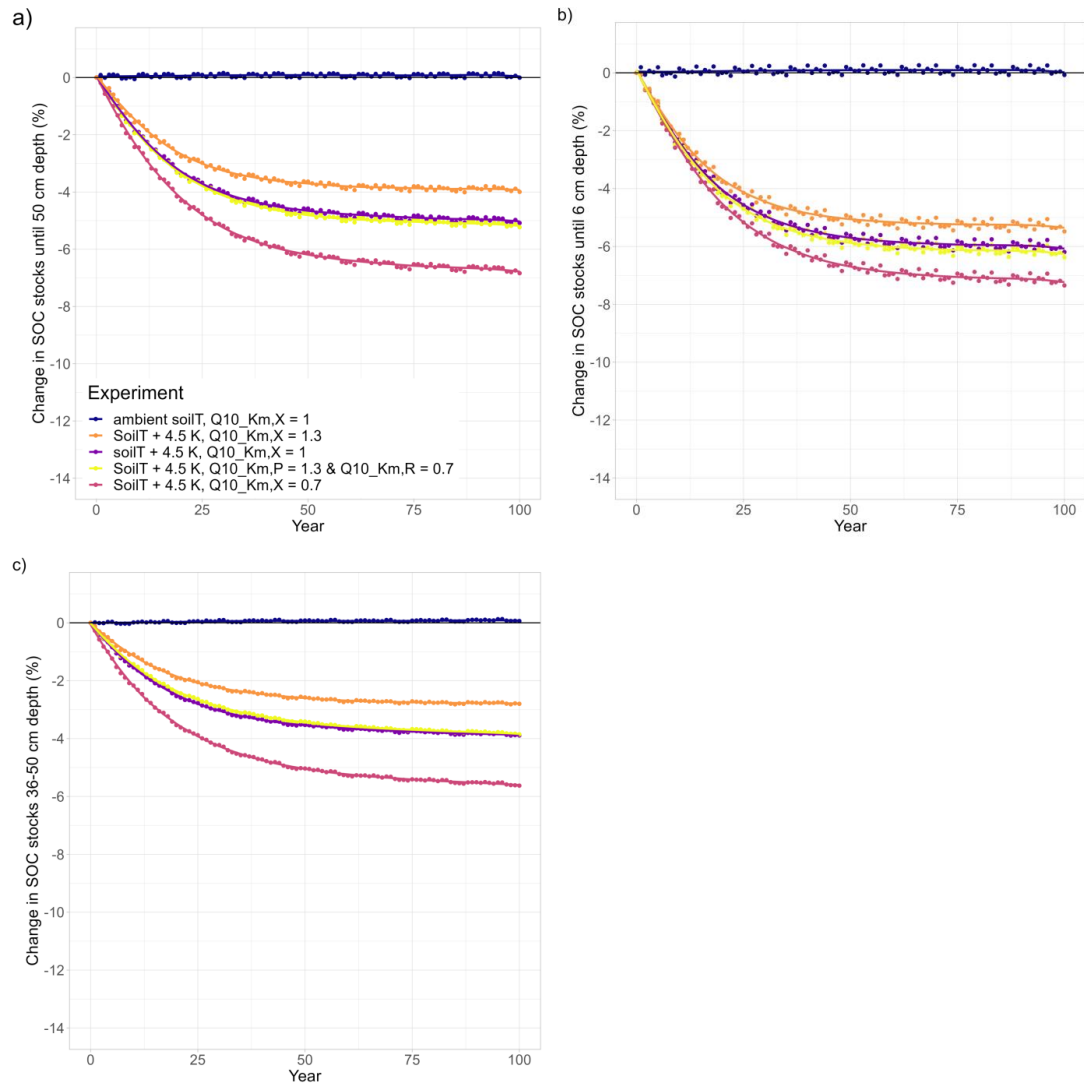
245 This indicates that in the subsoil, where microbial biomass is lower, the relative importance of $Q_{10,Km,X}$ is larger than in the topsoil.

Contrastingly, using a Q_{10} value for half-saturation constants $K_{m,P}$ and $K_{m,R}$ of 1.3 (reflecting the temperature sensitivity of the depolymerisation of the polymeric litter pool) counteracts the warming effect and reduces SOC losses from the soil. The result is still a net loss: SOC stocks in the top 50 cm deplete by 4%, with higher SOC losses from topsoil compared to the subsoil (- 5.5 and - 2.8%, respectively, Fig. 3, orange points). Similar to the model run where $Q_{10,Km,X}$ is 0.7, the temperature sensitivity of K_m in the model run where both $Q_{10,Km,P}$ and $K_{m,R}$ are 1.3 has a relatively larger impact in the subsoil than the topsoil.

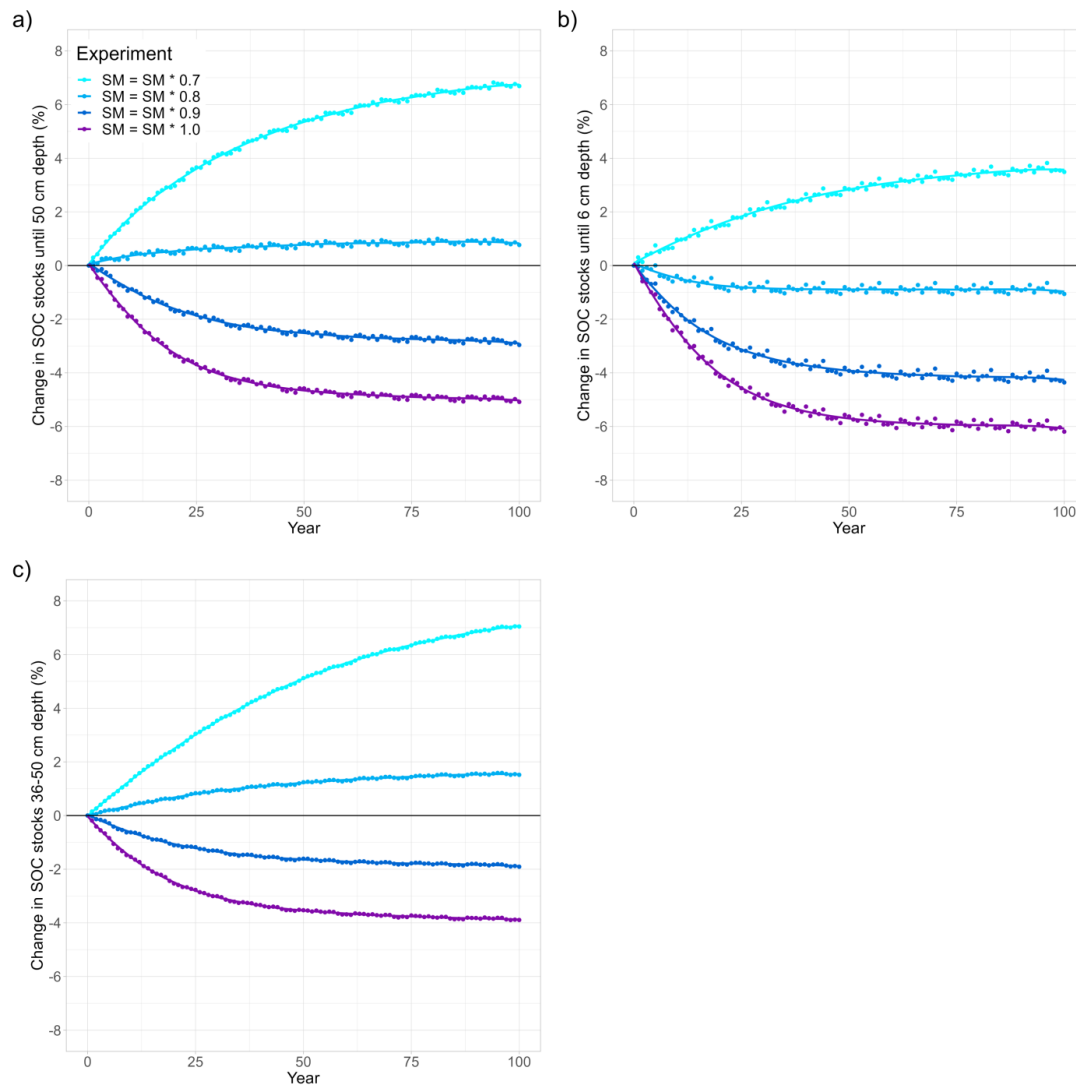
250 Using individual Q_{10} values for the half-saturation constant for the depolymerisation of microbial residues ($K_{m,R}$) of 0.7 and of 1.3 for the polymeric litter pool ($K_{m,P}$) results in SOC losses from the top 50 cm (- 5.2%, Fig.3, yellow). In comparison to the run where $Q_{10,Km,X} = 1$ this result is very similar (5.1% loss from warming alone), indicating that the opposing temperature sensitivities of depolymerisation of microbial residues and polymeric litter pool cancel each other out. The topsoil loses more SOC (- 6.4%) than the subsoil (- 3.9%), but in comparison the run where $Q_{10,Km,X} = 1$ the losses from the topsoil layer are slightly higher in the subsoil (-0.2%) similar in subsoil (0% difference).

3.2 Drought effects on SOC decomposition

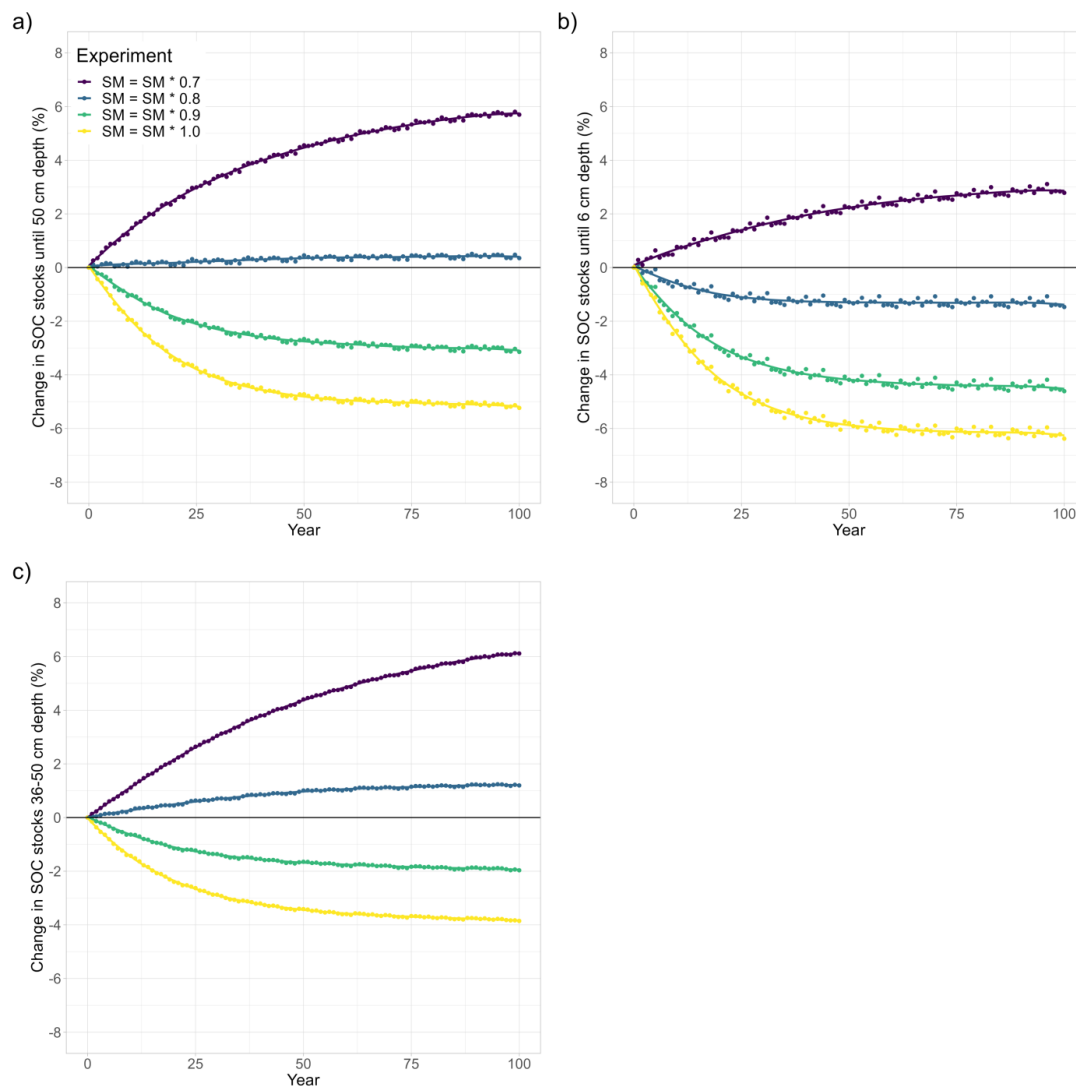
260 Inducing a drought strongly dampens the warming effect on SOC (Fig. 4). Depending on the drought intensity, the top 50 cm loses less SOC, or even acts as a sink and starts accumulating SOC over the course of the simulation period. A 10% reduction in SM results in a SOC loss of 3%, whereas at 80% and 70% SM, the soil column accumulates 1.0% or 6.8% SOC, respectively (Table 2). Stronger drought intensity led to a larger difference in modelled SOC stocks at 0-50 cm, from -5.1% at the original SM, to + 6.8% at 70% SM, a difference of 11.9 percentage points. This increased drought response on SOC decomposition is a direct result of the increase in the value of $f_{Km,X}(T_{soil}, \theta)$ with decreasing SM (θ , Eq. (4)). Again, the topsoil and subsoil layers show a different response: In the topsoil, there is high microbial biomass and therefore, the effect of the drought on microbial depolymerisation is not as strong as in the subsoil. Additionally, drought decreases the amount of MAOC in the subsoil, while POC accumulates (Fig. A1). As a result, the ratio of POC:MAOC increases, especially in the topsoil (Fig. A2). In 0 - 6 cm, SOC losses are 4.4% at 90% SM, 1.1% at 80% SM, and a 3.8% SOC gain at 70% SM. In the subsoil layer between 36 - 50 cm, there is a loss of 1.9% SOC at 90% SM, and 1.6% and 7.1% SOC gains at 80% and 70% SM, respectively. At 80% SM the drought has an opposite effect in the topsoil (a net source) than in the subsoil (a net sink). The whole column response, however, is a net sink, highlighting the strong contribution of the subsoil to the overall response.



275 **Figure 3: Temperature effects on long-term changes in modelled SOC stocks (% SOC lost since simulation year 0) for different model experiments in a) a whole soil column (0 - 50 cm), b) the topsoil layer (0 - 6 cm) and c) a subsoil layer (36 - 50 cm). In all runs, ambient SM (SM * 1.0) was used.**



280 **Figure 4: SM effects on long-term changes in modelled SOC stocks (% SOC lost since simulation year 0) for different model experiments in a) a whole soil column (0 - 50 cm), b) the topsoil layer (0 - 6 cm) and c) a subsoil layer (36 - 50 cm). Soil moisture is reduced in 10% steps from ambient (SM * 1.0) to 70% (SM * 0.7). In all runs, $Q_{10,Km,X} = 1$ (not temperature sensitive).**



285 **Figure 5: Combined temperature and SM effects on long-term changes in modelled SOC stocks (% SOC lost since simulation year 0) for different model experiments in a) a whole soil column (0 - 50 cm), b) the topsoil layer (0 - 6 cm) and c) a subsoil layer (36 - 50 cm). In all model runs, the soil was warmed by 4.5 K and $Q_{10,Km,P}$ was 1.3 for depolymerisation of litter and $Q_{10,Km,R}$ was 0.7 for depolymerisation of microbial residues.**



3.3 Combined effects of drought and temperature sensitivity of half-saturation constants on SOC decomposition

290 To investigate the potentially counteracting responses of temperature sensitivity of K_m and droughts, we also run the model for the three different drought intensities in conjunction with a $Q_{10,Km,P}$ value of 1.3 for the polymeric litter pool and a $Q_{10,Km,R}$ value of 0.7 for the microbial residues pool. At ambient SM conditions, the temperature sensitivity of both $K_{m,X}$ values only marginally amplified the warming effects (Figs. 3 and 5, yellow points). When SM is reduced, however, this slows down the decomposition rates (Fig. 5, Table 2): At a 10% reduction in available SM, less SOC is lost from the top 50 cm (-3.1%) than
295 when SM is kept at ambient levels (-5.2%). At 80 and 70% SM the soil starts gaining SOC (+0.5% and 5.8%, respectively). Generally, modelled SOC stocks for this combination of temperature sensitivities of K_m and different drought intensities closely resemble the simulated drought response (Fig. 4), with the temperature sensitivity of K_m counteracting the drought effects: when K_m is temperature sensitive, SOC losses are always higher, and SOC gains are always smaller than when K_m is not temperature sensitive (Table 2). Similar to the drought experiments (Section 3.2), the differences in modelled SOC stocks at 0-50 cm increase with stronger drought intensity. Interestingly, the temperature sensitivity effect through $Q_{10,Km,P}$ and $Q_{10,Km,R}$ also increases with stronger drought intensity: For example, at ambient SM, SOC stocks decreased by 5.1% when both $Q_{10,Km,X}$ are 1, and decreased by 5.2% when $Q_{10,Km,R} = 0.7$ and $Q_{10,Km,P} = 1.3$, a difference of 0.1 percentage point (Table 2). But at 70% SM, SOC stocks increase to 6.8% when both $Q_{10,Km,X}$ are 1, and increase to 5.8% when $Q_{10,Km,R} = 0.7$ and $Q_{10,Km,P} = 1.3$, a difference of 1.0 percentage point. The same trend is also visible for both the topsoil (relative difference
305 from 0.2 percentage point at SM = 1.0 to 0.7 percentage point difference at SM = 0.7) and the subsoil (no difference at SM = 1.0 to 1.0 percentage point difference at SM = 1.0). At the same time, the ratio POC:MAOC did not change much compared to the model run where $K_{m,X}$ was not temperature sensitive (Fig. A2, yellow and pink). This indicates that rather than causing a shift in the litter and microbial residues C pools, microbial limitation is strong under dry conditions (low C_B , Fig. 1), which in turn increases the importance of $Q_{10,Km,R}$ and $Q_{10,Km,P}$ for the overall SOC decomposition rates. Contrasting to the results
310 from the isolated warming and drought experiments, the differences in SOC stock changes between the topsoil and subsoil are not very large: From a -6.4% SOC loss to +3.1% SOC gain, which is a 9.5 percent point change in the topsoil, to -3.9 to +6.1, which is a 10 percentage point change in the subsoil (Table 2). These results indicate that the combined sensitivity of SOC stocks to moisture and temperature in topsoil and subsoil is similar due to the counteracting effects of temperature and soil moisture on K_m (Eq. (6)): higher temperatures promote SOC decomposition rates due to the stronger influence of depolymerisation of microbial residues (which has a $Q_{10,Km,R}$ value of 0.7), whereas drought decreases SOC decomposition
315 rates.

320 4 Discussion

4.1 Warming effects on SOC decomposition

We find that warming the soil by 4.5 K accelerates SOC losses, and these losses are proportionally higher in the topsoil than in the subsoil. This is expected, as higher soil temperature increase maximum depolymerisation rates and microbial growth rates through $Q_{10,Vmax,X}$ (Eq. (4)). Our findings are also consistent with other modelling studies that investigate isolated soil
325 warming effects (e.g. Pallandt et al., 2022; Todd-Brown et al., 2014; Wieder et al., 2018), as well as with results from a recent large meta-analysis of SOC profiles (Wang et al., 2022a), which reports higher losses of SOC stock and SOC content from topsoil (0-30 cm) than subsoils (0.3 - 1m). In our study, during the warming experiments, the topsoil almost always loses more



SOC than the subsoil, except when $Q_{10,Km,P}$ and $Q_{10,Km,R}$ are both set to 0.7 and SOC losses are accelerated in the subsoil (-5.6% loss). Two depth-dependent model processes play an important role in these top- and subsoil differences. Firstly, microbial biomass (C_b) decreases with depth, and as microbial biomass declines, the Michaelis-Menten term for depolymerisation decreases (Fig. 1, Eq. (3)), thereby limiting the depolymerisation rates at lower depths. Secondly, SOC is protected from microbial decomposition by sorption to mineral surfaces, and mineral-associated organic carbon (MAOC, consisting of adsorbed DOC and microbial residues) strongly increases with soil depth (Fig. A1). In JSM, the Q_{10} value of the mineral-associated C pools are 1.08 for adsorption and 1.34 for desorption, which is much lower than the Q_{10} values of the particulate organic carbon (POC) pools: The Q_{10} value for microbial depolymerisation of polymeric litter and microbial residues is 2.16, and 1.98 for microbial C uptake (Table 1, Allison et al., 2010; Wang et al., 2012, 2013). As the ratio of MAOC to POC strongly increases in the subsoil, this leads to an overall lower apparent temperature sensitivity of SOC pools in the subsoil. Total SOC losses consist of DOC, POC, and MAOC from the 36 - 50 cm subsoil layer, so the overall SOC losses may be relatively small as the majority of SOC in this layer consists of protected MAOC - which decreases its overall temperature sensitivity.

Whether or not the apparent temperature sensitivity of SOC declines with depth, as we observe in this study, is still a topic of debate. According to kinetic theory subsoils may have lower apparent Q_{10} values when they contain less complex, necromass derived substrates (Davidson and Janssens, 2006; Hicks Pries et al., 2023). Contrastingly, the same argument is used to explain higher temperature sensitivities in subsoils when they may contain molecules with higher activation energies (e.g. Li et al., 2020). These observed higher temperature sensitivities could be the result of deriving the apparent Q_{10} values from bulk soil samples containing both POC and MAOC, whereas several other studies demonstrated that this trend can be counteracted by the strong mineral protection of SOC in subsoils (Gentsch et al., 2018; Gillabel et al., 2010; Qin et al., 2019) and that reported high apparent Q_{10} values originate from the decomposition of POC (Soong et al., 2021). In a recent review, Hicks Pries et al. (2023) conclude that the temperature response of deep soils is likely to be context dependent, and that subsoils with high POC content, or with low reactive mineral content are likely to be more susceptible to warming than soils with limited POC or with highly reactive mineral surfaces which protect SOC from microbial decomposition. In our model experiments, MAOC strongly increased with soil depth, which resulted in smaller total SOC losses from the topsoil than the subsoil layer in response to warming.

We observe stronger model responses to different $Q_{10,Km,X}$ values in subsoils than in topsoils, firstly, because microbial limitation is stronger in subsoils than in topsoils. At low microbial biomass (C_b), the value of $K_{m,X}$ becomes increasingly important (Fig. 1, Eq. (3)). At the same time, depolymerisation rates only affect the POC pools (C_p and C_r) and not the MAOC pools (adsorbed DOC and adsorbed microbial residues). Since the ratio of POC:MAOC is low in subsoils (Fig. A2), the total SOC losses from subsoils are lower from the subsoil than the topsoil, despite the higher sensitivity to different $Q_{10,Km,X}$ values. So, when $Q_{10,Km,X} < 1$, SOC losses can be further accelerated, especially in the deep soil. In our study, this lower Q_{10} was associated with the breakdown of proteins from the microbial residues pool. The contribution of microbial residues in the deep soil to total SOC is highly significant and can be up to 54% in grasslands (Wang et al., 2021). So if free POC in deep soils is indeed more sensitive to warming as a result of low microbial biomass, our model results support the finding that deep soils rich in microbial residues are more temperature sensitive than those that contain less microbially-derived POC contents, due to the lower $Q_{10,Km}$ value of the breakdown of polypeptides. However, compared to plant-derived POC, microbial residues have a high mineral sorption potential (Liu et al., preprint; Buckeridge et al., 2022) and could therefore be more protected from decomposition.



4.2 Drought effects on SOC decomposition

Our results show that soil drying can alleviate the losses of SOC from soil warming. In our model, this is the result of the soil
370 moisture sensitivity of the half-saturation constants for microbial depolymerisation ($K_{m,R}$ and $K_{m,P}$, Eq. (6)): Lower soil
moisture reduces the Michaelis-Menten term for depolymerisation (Fig. 1), which lowers the SOC decomposition rates.
Microbial C uptake for growth is also sensitive to changes in soil moisture through changes in the air-filled pore space (Eqs. 7
and 8), but this would result in faster SOC decomposition rates as microbial growth is less affected by oxygen limitation, which
was not the case for any of the modelled drought experiments. Generally, SOC decomposition peaks at intermediate soil
375 moisture, but most soils are below these optimal soil moisture levels and as a result, drying leads to reduced decomposition
rates due to stronger microbial limitation, whereas wetting the soil leads to an acceleration of the decomposition rates until
oxygen limitation limits SOC decomposition rates (Davidson et al., 2012; Moyano et al., 2018; Pallandt et al., 2022; Skopp et
al., 1990). In our model framework, substrate and oxygen limitation is split between two processes: we simulate moisture-
driven diffusion limitation on the microbial depolymerisation rates (reverse MM-kinetics, Eq. (6)), and oxygen and DOC
380 availability affect microbial growth (forward MM-kinetics, Eq. (7)). We found that soil drying consistently reduced modelled
SOC losses compared to SOC losses due to soil warming alone, indicating that microbial limitation of depolymerisation is
more important than oxygen limitation on microbial growth in our study. Additional support for strong microbial limitation on
SOC decomposition comes from our observation that particulate organic C (POC) accumulates in both the topsoil and subsoil
layers in response to the most intense drought scenario ($SM = SM * 0.7$, Fig. A1). If microbes were not limited by the drought,
385 they would degrade POC quickly in response to warming.

Our finding that microbial SOC decomposition consistently declines in response to drought is in agreement with other studies
that explore drought effects on SOC decomposition using microbially explicit models (Liang et al., 2021; Wang et al., 2020;
Zhang et al., 2022). In the topsoil, we find that the impact of each 10% reduction in SM has a relatively small impact on
alleviating SOC losses through warming, compared to the subsoil (Fig. 4). These observed differences in the drought response
390 between top- and subsoil can mainly be explained by the vertical differences in microbial biomass concentration (C_B), which
is higher in the topsoil than the subsoil. Therefore, at low C_B , the relative impact of drought on the MM-term for
depolymerisation is larger in the subsoil than the topsoil, making the modelled subsoil SOC stocks more sensitive to drought.
For example, at 80% SM, modelled SOC stocks in the topsoil reduce in response to soil warming (from -6.2% to -1.1% as SM
reduces to 80%, a net difference of 5.1 percent points), whereas subsoil SOC stocks decrease at ambient SM but increase at
395 80% SM (from -3.9% to +1.6%, a difference of 5.5 percent points). As discussed in section 4.1, the relatively higher sensitivity
of the subsoil to not only warming but also to drought, is also related to the strong increase in MAOC with depth and its lower
temperature sensitivity compared to that of the POC pools. In order to focus completely on drought effects on microbial SOC
decomposition, adsorption and desorption rates were not sensitive to changes in soil moisture during our experiments. Drought
favours the stabilisation of SOC on mineral surfaces (Blankinship and Schimel, 2018), thereby protecting it from microbial
400 depolymerisation. Therefore, if we would consider the moisture sensitivity of adsorption and desorption rates in our model,
we expect a further decrease in the SOC decomposition rates in response to drought. The formulation of moisture sensitivity
of adsorption and desorption, however, is not well established to our knowledge.

Overall, our model results indicate a potential for net SOC gains in 0 - 50 cm depth when SM is reduced to 80% or 70% of its
original values, and that a large part of the whole soil column response is driven by the subsoil. While data-driven deep soil
405 drying studies are rare, our simulation results are supported by a recent study (Brunn et al., 2023), where total annual
precipitation throughfall was reduced by 70% for 5 consecutive years and both SOC stocks and SOC stability increased
between 0 - 30 cm. They found that the majority of the SOC stock increase occurred in the top 5 cm as a result of higher root
exudates, but we do not consider this in our experiment. We found that the largest SOC stock increase occurred in the subsoil,



because of the higher sensitivity of subsoil to drought at low microbial biomass concentrations and the strong protection of
410 MAOC from microbial depolymerisation. Our finding that SOC stocks can potentially increase with drought despite the
expected losses through warming, is mainly the result of lower microbial depolymerisation (Eq. (6), Fig. 1). Indeed, short term
studies indicate that SOC stocks may increase under drought, as a strong reduction in microbial activity may dominate over
the effect of reduced litter and root inputs (Brunn et al., 2023; Deng et al., 2021; Moyano et al., 2013). While results from
short-term data-driven studies support our modelling results, long-term drought studies generally show a decline in SOC
415 stocks, which can be mainly attributed to the effects of soil warming and decreased litter inputs (e.g. Deng et al., 2021; Meier
and Leuschner, 2010). An advantage of our stand-alone soil model environment with prescribed litter inputs is that it allows
us to individually test soil warming and drying effects on long-term SOC stocks, while eliminating the potentially confounding
effects from changes in plant productivity. Recent research has shown that the chances of drought coinciding with high soil
temperatures will further increase in the future (García-García et al., 2023). As a result, the counteracting effects of K_m and
420 drought may be at their strongest, and ecosystems dominated by infrequent moisture inputs may show strong sensitivities to
soil warming and drought.

4.3 Combined effects of drought and temperature sensitivity of half-saturation constants on SOC decomposition

We show that soil drying in combination with temperature sensitivity of the half-saturation constants for depolymerisation of
polymeric litter and microbial residues, can both increase or decrease SOC stocks, and that the direction and magnitude of the
425 effect on SOC stocks depends on drought intensity. The combined effects of soil drying and temperature sensitivity of the half-
saturation constants for depolymerisation on SOC stocks closely resembled that of the drought response, which indicates that
microbial limitation on depolymerisation poses a strong control on modelled SOC stocks and that drought can indeed alleviate
SOC losses in response to soil warming. While the effect of drought on modelled SOC stocks is strong, the temperature
sensitivity of $K_{m,x}$ can counteract these effects: Compared to the model runs without temperature sensitivity of $K_{m,x}$, SOC
430 losses are higher and SOC gains are smaller. This indicates that the breakdown of microbial residues, which had a $Q_{10,Km,R}$
value of 0.7, is important for the overall results because a Q_{10} value lower than 1 increases the MM-term for depolymerisation,
and accelerates SOC decomposition. Furthermore, this counteracting effect of $Q_{10,Km,x}$ is stronger with increased drought
intensity while the ratio POC:MAOC does not change much when compared to the model run where $Q_{10,Km,x}$ is not
temperature sensitive. In line with our results from the isolated drought experiments (Section 4.2), this supports the conclusion
435 that microbial limitation increases under drought, so that $Q_{10,Km,x}$ becomes more important for the overall depolymerisation
rates.

Unlike the individual warming and drought experiments, we only find small differences in SOC stock changes between the
top- and subsoil for the combination of drought and temperature sensitivity of $K_{m,R}$ and $K_{m,P}$. This shows that drought and
temperature sensitivity can both play a strong role, and counteract each other so that the overall changes in SOC stocks appear
440 similar. This is an important result, because long-term warming can accelerate soil drying, especially at the soil surface (Berg
and Sheffield, 2018; Fan et al., 2022; García-García et al., 2023). Our results show divergent responses of top and subsoil SOC
stocks to concurrent soil warming and drying, in particular at a 20% SM reduction, where modelled SOC stocks in the topsoil
increase but decrease in the subsoil. While we only explored the effects of evenly drying out the soil column in this study, the
long-term response of SOC stocks to soil moisture changes could be even more non-linear as top- and subsoils may not dry
445 out evenly (Berg et al., 2017). Using multi-model predictions, Berg et al. (2017) show that surface soil moisture decreases by
the end of the century, while subsoils, especially in the northern hemisphere, diverge with either less severe drying or wetter
conditions. On top of soil warming, such dynamic vertical changes in soil moisture have a strong potential of further
accelerating or slowing down SOC decomposition rates in the deep soil by microbial limitation or oxygen diffusion limitation



(Pallandt et al., 2022). We call for modelling studies that address such changes simultaneously by running ‘new generation’
450 models with future climate forcing datasets.

4.4 Microbial response to substrate changes in the POC/MAOC framework

The duration of our experiments is 100 simulation years, but the values of $Q_{10,Vmax}$ and $Q_{10,Km,X}$ may not stay constant over
time, as the environment changes and microbial communities adapt. However, in light of our long-term warming experiments
we feel confident with the choice of $Q_{10,Km}$ values, as they were measured in microorganisms that showed no sensitivity to a
455 6 °C increase in average temperature - but did show a strong response to changes in substrate types (Allison et al., 2018a). In
our model experiment, microbes have access to both litter inputs and microbial residues to depolymerise, which have
counteracting $Q_{10,Km}$ values and therefore the possibility to simultaneously accelerate and slow down microbial SOC
decomposition rates. In this light, it is important that modellers have access to data sources that help connect model Q_{10} values
460 for $K_{m,X}$ and V_{max} to the dominant C sources that microbes could depolymerise. For example, information on soils that are
high in POC versus soils that are high in MAOC: Soils with high MAOC contents and low POC inputs can have lower apparent
 Q_{10} values because $Q_{10,sorption}$ is much lower than the Q_{10} values of unprotected organic carbon (Table 1; Wang et al., 2012,
2013). Secondly, such soils would have necromass rather than fresh litter inputs as the dominant C substrate for microbes.
New datasets such as global maps of necromass C contributions to total SOC stocks (e.g. Liu et al., preprint) can inform
465 modellers on substrate type or SOC stabilisation mechanisms, and thereby help identify the climate sensitivities of SOC stocks
in different regions of the world. At the moment, though, there are no clear answers as to which values we should use for
 $Q_{10,Km,X}$ because SOC consists of many different molecules, which all have their own specific temperature sensitivities
(Allison et al., 2018b). One possibility to investigate the potential climate-substrate feedbacks with a model like JSM, would
be a further partitioning of the litter pools into functional groups related to their main degrading enzymes. Our current study,
which explores different values for $Q_{10,Km,X}$ already provides valuable insights into what might be possible. For example, soils
470 with high POC contents, i.e. with a developed organic layer as a result of high litter inputs, low SOC losses and low
bioturbation, are likely to have $Q_{10,Km,X}$ values > 1 , which has the potential to counteract soil warming effects through
 $Q_{10,Vmax}$, especially in deeper layers where microbial biomass is low and the temperature sensitivity of the half-saturation
constant will have a stronger impact. In combination with soil drought, this would further enhance microbial limitation for
depolymerisation and could dampen SOC losses in such organic soil layers over time - if litter inputs stay constant over time.
475 Peat soils could be an exception, as they usually have high volumetric water contents and drought can lift oxygen limitation,
thereby increasing SOC decomposition rates. It can be expected though, that long-term soil drying reduces root and leaf litter
inputs as plant productivity decreases (Deng et al., 2021). Therefore, we recommend future research focuses on further studying
climate-substrate interactions within a fully coupled soil-plant model, such as the coupling between land surface model
QUINCY (Thum et al., 2019) with JSM, which is nearing completion.

480 5 Conclusions

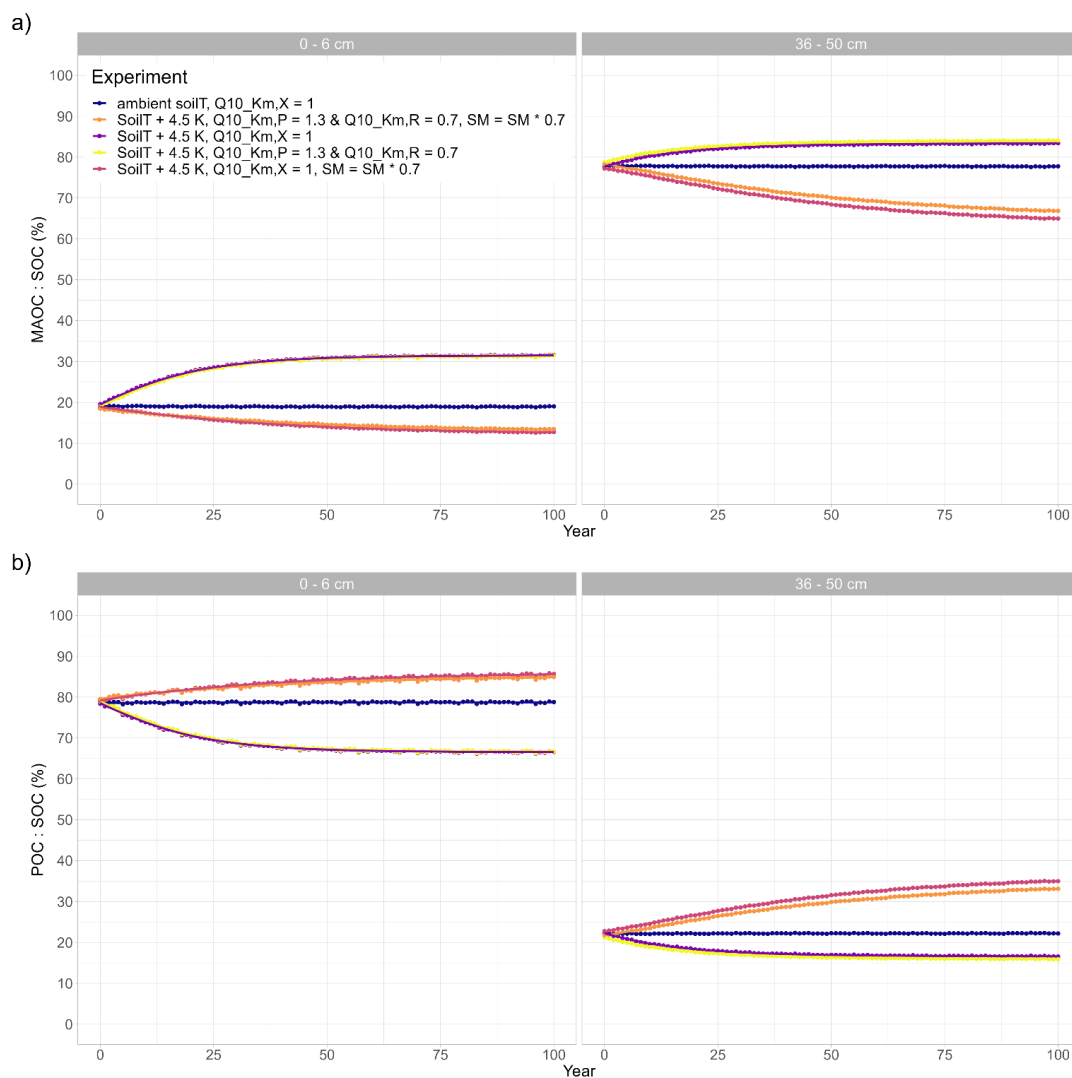
With JSM we show that both soil drying and warming pose strong controls on SOC decomposition. The vertically explicit
model structure allows us to demonstrate that subsoil SOC stocks respond differently to warming and drought through a
combination of processes. First of all, we show that SOC association to mineral surfaces plays an important role in reducing
the overall sensitivity of SOC stocks to microbial decomposition: MAOC strongly increases with soil depth and has a low
485 apparent temperature sensitivity, which results in smaller total SOC losses from the subsoil than the topsoil. At the same time,
our model results indicate that unprotected subsoil SOC is more sensitive to soil warming and drought. Secondly, we show
that drought can alleviate the effects of soil warming through microbial limitation on depolymerisation rates. As drought gets
stronger, microbially mediated depolymerisation rates become severely limited so that less SOC is lost from the soil. In the



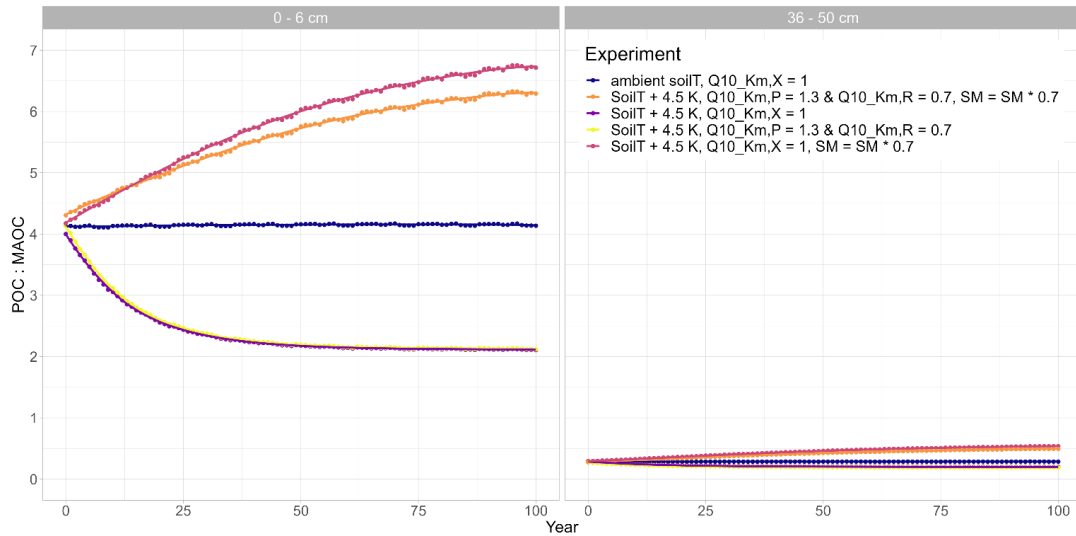
490 model experiments with constant litter inputs in this study this can even lead to SOC accumulation over time, despite soil
warming. Thirdly, we show that considering the temperature sensitivities of the half-saturation constants for different C
substrates (litter and microbial residues) is important, as they can both slow down and accelerate microbial SOC decomposition
rates. Our results highlight the importance of representing SOC decomposition processes in a vertically resolved model, which
includes carbon stabilisation on mineral surfaces. We recommend that future model development focuses on further identifying
the (un)importance of temperature sensitivities of V_{max} and $K_{m,X}$ for different C substrates and moisture sensitivities of all
495 microbial-mineral interactions in the new class of soil organic carbon models.



Appendix A



500 **Figure A1:** a) Ratio of mineral associated organic carbon (MAOC) to SOC (%) and b) particular organic carbon (POC) to SOC (%) for different model runs at two different soil depths: Topsoil (0 - 6 cm) and subsoil (36-50 cm). If not indicated otherwise, SM = SM * 1.0 in the experiment.



505 **Figure A2: Ratio of particular organic carbon (POC) to mineral-associated carbon (MAOC) for different model runs at two different soil depths: Topsoil (0 - 6 cm) and subsoil (36-50 cm). If not indicated otherwise, $SM = SM * 1.0$ in the experiment.**



Code availability

The Jena Soil Model (JSM) - release01 is fully described and published under <https://doi.org/10.5194/gmd-13-783-2020>. The JSM source code is available online (<https://git.bgc-jena.mpg.de/quincy/quincy-model-releases>, branch “jasm/release01”), but access is restricted to registered users. Readers interested in running the model should request a username and password from S. Zaehle or via the git repository. JSM is developed using the framework of the QUINCY model. The QUINCY model is free software: It can be distributed and/or modified under the terms of the GNU GPL version 3 (<https://www.gnu.org/licenses/gpl-3.0.en.html>, last access 10 January 2024). The use of the QUINCY model relies on the application of software developed by the MPI for Meteorology, which is subject to the MPI-M ICON software licence (see ICON section: “By using ICON, the user accepts the individual licence (<https://code.mpimet.mpg.de/attachments/download/20888/MPI-M-ICONLizenzvertragV2.6.pdf>, last access 10 January 2024). Where software is supplied by third parties such as the MPI for Meteorology, it is indicated in the header of the file. Model users are strongly encouraged to follow the fair-use policy stated at <https://www.bgc-jena.mpg.de/en/bsi/projects/quincy/software> (last access: 10 January 2024).

Author contribution

MP wrote the original draft for the manuscript with contributions from all co-authors. BA and LY wrote the original JSM model code (version 1.0, see code availability), MP and BA wrote minor code modifications to run the model experiments as described in Section 2, and MP performed the model simulations and created all visualisations. This study was conceptualised by MP, BA, MS, and HL. Formal analysis was carried out by MP and BA. Funding acquisition: BA, HL and MR. Supervision of MP by BA, HL, MS, and MR.

Acknowledgements

MP is grateful for discussions with Prof. S. Zaehle in the early phases of this study as well as technical support from J. Nabel and J. Engel from the QUINCY modelling team at the Max Planck Institute for Biogeochemistry in Jena. MP received funding support for this work from the Norwegian Research Council through grant no. RCN 255 061 (MOisture dynamics and CArbon sequestration in BOREal Soils) and the Max Planck Institute for Biogeochemistry.

Competing interests

The authors declare that they have no conflict of interest.

References

- Abramoff, R., Davidson, E., and Finzi, A. C.: A parsimonious modular approach to building a mechanistic belowground carbon and nitrogen model, *Journal of Geophysical Research: Biogeosciences*, 122, 2418–2434, <https://doi.org/doi:10.1002/2017JG003796>, 2017.
- Ahrens, B., Braakhekke, M. C., Guggenberger, G., Schrumppf, M., and Reichstein, M.: Contribution of sorption, DOC transport and microbial interactions to the ¹⁴C age of a soil organic carbon profile: Insights from a calibrated process model, *Soil Biology and Biochemistry*, 88, 390–402, <https://doi.org/10.1016/j.soilbio.2015.06.008>, 2015.
- Ahrens, B., Guggenberger, G., Rethemeyer, J., John, S., Marschner, B., Heinze, S., Angst, G., Mueller, C. W., Kögel-Knabner, I., Leuschner, C., Hertel, D., Bachmann, J., Reichstein, M., and Schrumppf, M.: Combination of energy limitation and sorption capacity explains ¹⁴C depth gradients, *Soil Biology and Biochemistry*, 148, 107912, <https://doi.org/10.1016/j.soilbio.2020.107912>, 2020.



- Allison, S. D., Wallenstein, M. D., and Bradford, M. A.: Soil-carbon response to warming dependent on microbial physiology, *Nature Geoscience*, 3, 336, <https://doi.org/10.1038/ngeo846> [https://www.nature.com/articles/ngeo846#supplementary-](https://www.nature.com/articles/ngeo846#supplementary-information)
545 information, 2010.
- Allison, S. D., Romero-Olivares, A. L., Lu, L., Taylor, J. W., and Treseder, K. K.: Temperature acclimation and adaptation of enzyme physiology in *Neurospora discreta*, *Fungal Ecology*, 35, 78–86, <https://doi.org/10.1016/j.funeco.2018.07.005>, 2018a.
- Allison, S. D., Romero-Olivares, A. L., Lu, Y., Taylor, J. W., and Treseder, K. K.: Temperature sensitivities of extracellular enzyme Vmax and Km across thermal environments, *Glob Chang Biol*, 24, 2884–2897, <https://doi.org/10.1111/gcb.14045>,
550 2018b.
- Berg, A. and Sheffield, J.: Climate Change and Drought: the Soil Moisture Perspective, *Curr Clim Change Rep*, 4, 180–191, <https://doi.org/10.1007/s40641-018-0095-0>, 2018.
- Berg, A., Sheffield, J., and Milly, P. C. D.: Divergent surface and total soil moisture projections under global warming, *Geophysical Research Letters*, 44, 236–244, <https://doi.org/10.1002/2016GL071921>, 2017.
- 555 Blankinship, J. C. and Schimel, J. P.: Biotic versus Abiotic Controls on Bioavailable Soil Organic Carbon, *Soil Systems*, 2, 10, <https://doi.org/10.3390/soilsystems2010010>, 2018.
- Braakhekke, M. C., Beer, C., Hoosbeek, M. R., Reichstein, M., Kruijt, B., Schrumpf, M., and Kabat, P.: SOMPROF: A vertically explicit soil organic matter model, *Ecological Modelling*, 222, 1712–1730, <https://doi.org/10.1016/j.ecolmodel.2011.02.015>, 2011.
- 560 Brunn, M., Krüger, J., and Lang, F.: Experimental drought increased the belowground sink strength towards higher topsoil organic carbon stocks in a temperate mature forest, *Geoderma*, 431, 116356, <https://doi.org/10.1016/j.geoderma.2023.116356>, 2023.
- Buckeridge, K. M., Mason, K. E., Ostle, N., McNamara, N. P., Grant, H. K., and Whitaker, J.: Microbial necromass carbon and nitrogen persistence are decoupled in agricultural grassland soils, *Commun Earth Environ*, 3, 1–10, <https://doi.org/10.1038/s43247-022-00439-0>, 2022.
- 565 Cook, B. I., Mankin, J. S., Marvel, K., Williams, A. P., Smerdon, J. E., and Anchukaitis, K. J.: Twenty-First Century Drought Projections in the CMIP6 Forcing Scenarios, *Earth’s Future*, 8, e2019EF001461, <https://doi.org/10.1029/2019EF001461>, 2020.
- Cotrufo, M. F. and Lavelle, J. M.: Chapter One - Soil organic matter formation, persistence, and functioning: A synthesis of current understanding to inform its conservation and regeneration, in: *Advances in Agronomy*, vol. 172, edited by: Sparks, D. L., Academic Press, 1–66, <https://doi.org/10.1016/bs.agron.2021.11.002>, 2022.
- Cotrufo, M. F., Wallenstein, M. D., Boot, C. M., Deneff, K., and Paul, E.: The Microbial Efficiency-Matrix Stabilization (MEMS) framework integrates plant litter decomposition with soil organic matter stabilization: do labile plant inputs form stable soil organic matter?, *Global Change Biology*, 19, 988–995, <https://doi.org/10.1111/gcb.12113>, 2013.
- 575 Davidson, E. A. and Janssens, I. A.: Temperature sensitivity of soil carbon decomposition and feedbacks to climate change, *Nature*, 440, 165, <https://doi.org/10.1038/nature04514>, 2006.
- Davidson, E. A., Janssens, I. A., and Luo, Y.: On the variability of respiration in terrestrial ecosystems: moving beyond Q10, *Global Change Biology*, 12, 154–164, <https://doi.org/10.1111/j.1365-2486.2005.01065.x>, 2006.
- Davidson, E. A., Sudeep, S., Samantha, S. C., and Savage, K.: The Dual Arrhenius and Michaelis–Menten kinetics model for decomposition of soil organic matter at hourly to seasonal time scales, *Global Change Biology*, 18, 371–384, <https://doi.org/doi:10.1111/j.1365-2486.2011.02546.x>, 2012.
- 580 Deng, L., Peng, C., Kim, D.-G., Li, J., Liu, Y., Hai, X., Liu, Q., Huang, C., Shanguan, Z., and Kuzyakov, Y.: Drought effects on soil carbon and nitrogen dynamics in global natural ecosystems, *Earth-Science Reviews*, 214, 103501, <https://doi.org/10.1016/j.earscirev.2020.103501>, 2021.



- 585 Dwivedi, D., Riley, W. J., Torn, M. S., Spycher, N., Maggi, F., and Tang, J. Y.: Mineral properties, microbes, transport, and plant-input profiles control vertical distribution and age of soil carbon stocks, *Soil Biology and Biochemistry*, 107, 244–259, <https://doi.org/10.1016/j.soilbio.2016.12.019>, 2017.
- Fan, K., Slater, L., Zhang, Q., Sheffield, J., Gentile, P., Sun, S., and Wu, W.: Climate warming accelerates surface soil moisture drying in the Yellow River Basin, China, *Journal of Hydrology*, 615, 128735, <https://doi.org/10.1016/j.jhydrol.2022.128735>, 2022.
- 590 García-García, A., Cuesta-Valero, F. J., Miralles, D. G., Mahecha, M. D., Quaas, J., Reichstein, M., Zscheischler, J., and Peng, J.: Soil heat extremes can outpace air temperature extremes, *Nat. Clim. Chang.*, 13, 1237–1241, <https://doi.org/10.1038/s41558-023-01812-3>, 2023.
- Garnier, S., Ross, N., BoB Rudis, Filipovic-Pierucci, A., Galili, T., Timelyportfolio, O’Callaghan, A., Greenwell, B., Sievert, C., Harris, D. J., Sciaini, M., and JJ Chen: `sjmgarnier/viridis`: CRAN release v0.6.3, <https://doi.org/10.5281/ZENODO.4679423>, 2023.
- 600 Gentsch, N., Wild, B., Mikutta, R., Čapek, P., Diáková, K., Schrupf, M., Turner, S., Minnich, C., Schaarschmidt, F., Shibistova, O., Schnecker, J., Urich, T., Gittel, A., Šantrůčková, H., Bárta, J., Lashchinskiy, N., Fuß, R., Richter, A., and Guggenberger, G.: Temperature response of permafrost soil carbon is attenuated by mineral protection, *Global Change Biology*, 24, 3401–3415, <https://doi.org/10.1111/gcb.14316>, 2018.
- Gillabel, J., Cebrian-Lopez, B., Six, J., and Merckx, R.: Experimental evidence for the attenuating effect of SOM protection on temperature sensitivity of SOM decomposition, *Global Change Biology*, 16, 2789–2798, <https://doi.org/10.1111/j.1365-2486.2009.02132.x>, 2010.
- Hicks Pries, C., Ryals, R., Zhu, B., Min, K., Cooper, A., Goldsmith, S., Pett-Ridge, J., Torn, M., and Asefaw Berhe, A.: The Deep Soil Organic Carbon Response to Global Change, *Annual Review of Ecology, Evolution, and Systematics*, 54, null, <https://doi.org/10.1146/annurev-ecolsys-102320-085332>, 2023.
- Hsu, H. and Dirmeyer, P. A.: Uncertainty in Projected Critical Soil Moisture Values in CMIP6 Affects the Interpretation of a More Moisture-Limited World, *Earth’s Future*, 11, e2023EF003511, <https://doi.org/10.1029/2023EF003511>, 2023.
- 610 Kallenbach, C. M., Frey, S. D., and Grandy, A. S.: Direct evidence for microbial-derived soil organic matter formation and its ecophysiological controls, *Nat Commun*, 7, 13630, <https://doi.org/10.1038/ncomms13630>, 2016.
- Koven, C. D., Riley, W. J., Subin, Z. M., Tang, J. Y., Torn, M. S., Collins, W. D., Bonan, G. B., Lawrence, D. M., and Swenson, S. C.: The effect of vertically resolved soil biogeochemistry and alternate soil C and N models on C dynamics of CLM4, *Biogeosciences*, 10, 7109–7131, <https://doi.org/10.5194/bg-10-7109-2013>, 2013.
- Koven, C. D., Hugelius, G., Lawrence, D. M., and Wieder, W. R.: Higher climatological temperature sensitivity of soil carbon in cold than warm climates, *Nature Climate Change*, 7, 817–822, <https://doi.org/10.1038/nclimate3421>, 2017.
- 615 Li, J., Pei, J., Pendall, E., Reich, P. B., Noh, N. J., Li, B., Fang, C., and Nie, M.: Rising Temperature May Trigger Deep Soil Carbon Loss Across Forest Ecosystems, *Advanced Science*, 7, 2001242, <https://doi.org/10.1002/advs.202001242>, 2020.
- Liang, C., Schimel, J. P., and Jastrow, J. D.: The importance of anabolism in microbial control over soil carbon storage, *Nat Microbiol*, 2, 1–6, <https://doi.org/10.1038/nmicrobiol.2017.105>, 2017.
- 620 Liang, J., Wang, G., Singh, S., Jagadamma, S., Gu, L., Schadt, C. W., Wood, J. D., Hanson, P. J., and Mayes, M. A.: Intensified Soil Moisture Extremes Decrease Soil Organic Carbon Decomposition: A Mechanistic Modeling Analysis, *Journal of Geophysical Research: Biogeosciences*, 126, e2021JG006392, <https://doi.org/10.1029/2021JG006392>, 2021.
- Liu, Y., Tian, J., He, N., and Tiemann, L.: Global microbial necromass contribution to soil organic matter, <https://doi.org/10.21203/rs.3.rs-473688/v1>, preprint.
- 625 Meier, I. C. and Leuschner, C.: Variation of soil and biomass carbon pools in beech forests across a precipitation gradient, *Global Change Biology*, 16, 1035–1045, <https://doi.org/10.1111/j.1365-2486.2009.02074.x>, 2010.



- Moyano, F. E., Manzoni, S., and Chenu, C.: Responses of soil heterotrophic respiration to moisture availability: An exploration of processes and models, *Soil Biology and Biochemistry*, 59, 72–85, <https://doi.org/10.1016/j.soilbio.2013.01.002>, 2013.
- Moyano, F. E., Vasilyeva, N., and Menichetti, L.: Diffusion limitations and Michaelis–Menten kinetics as drivers of combined
630 temperature and moisture effects on carbon fluxes of mineral soils, *Biogeosciences*, 15, 5031–5045,
<https://doi.org/10.5194/bg-15-5031-2018>, 2018.
- Pallandt, M., Ahrens, B., Koirala, S., Lange, H., Reichstein, M., Schrumpp, M., and Zaehle, S.: Vertically Divergent Responses
of SOC Decomposition to Soil Moisture in a Changing Climate, *JGR Biogeosciences*, 127,
<https://doi.org/10.1029/2021JG006684>, 2022.
- 635 Parton, W. J., Schimel, D. S., Cole, C. V., and Ojima, D. S.: Analysis of Factors Controlling Soil Organic Matter Levels in
Great Plains Grasslands, *Soil Science Society of America Journal*, 51, 1173–1179,
<https://doi.org/10.2136/sssaj1987.03615995005100050015x>, 1987.
- Parton, W. J., Scurlock, J. M. O., Ojima, D. S., Gilmanov, T. G., Scholes, R. J., Schimel, D. S., Kirchner, T., Menaut, J.-C.,
Seastedt, T., Garcia Moya, E., Kamnalrut, A., and Kinyamario, J. I.: Observations and modeling of biomass and soil organic
640 matter dynamics for the grassland biome worldwide, *Global Biogeochemical Cycles*, 7, 785–809,
<https://doi.org/10.1029/93GB02042>, 1993.
- Qin, S., Chen, L., Fang, K., Zhang, Q., Wang, J., Liu, F., Yu, J., and Yang, Y.: Temperature sensitivity of SOM decomposition
governed by aggregate protection and microbial communities, *Science Advances*, 5, eaau1218,
<https://doi.org/10.1126/sciadv.aau1218>, 2019.
- 645 R Core Team: R: A Language and Environment for Statistical Computing, 2023.
- RStudio Team: Rstudio: Integrated development environment for R., 2018.
- Sierra, C. A., Trumbore, S. E., Davidson, E. A., Vicca, S., and Janssens, I.: Sensitivity of decomposition rates of soil organic
matter with respect to simultaneous changes in temperature and moisture, *Journal of Advances in Modeling Earth Systems*, 7,
335–356, <https://doi.org/10.1002/2014MS000358>, 2015.
- 650 Skopp, J., Jawson, M. D., and Doran, J. W.: Steady-state aerobic microbial activity as a function of soil water content, *Soil
Science Society of America Journal*, 54, 1619–1625, <https://doi.org/10.2136/sssaj1990.03615995005400060018x>, 1990.
- Sokol, N. W., Whalen, E. D., Jilling, A., Kallenbach, C., Pett-Ridge, J., and Georgiou, K.: Global distribution, formation and
fate of mineral-associated soil organic matter under a changing climate: A trait-based perspective, *Functional Ecology*, 36,
1411–1429, <https://doi.org/10.1111/1365-2435.14040>, 2022.
- 655 Soong, J. L., Phillips, C. L., Ledna, C., Koven, C. D., and Torn, M. S.: CMIP5 Models Predict Rapid and Deep Soil Warming
Over the 21st Century, *Journal of Geophysical Research: Biogeosciences*, 125, e2019JG005266,
<https://doi.org/10.1029/2019JG005266>, 2020.
- Soong, J. L., Castanha, C., Hicks Pries, C. E., Ofiti, N., Porras, R. C., Riley, W. J., Schmidt, M. W. I., and Torn, M. S.: Five
years of whole-soil warming led to loss of subsoil carbon stocks and increased CO₂ efflux, *Science Advances*, 7, eabd1343,
660 <https://doi.org/10.1126/sciadv.abd1343>, 2021.
- Sulman, B. N., Phillips, R. P., Oishi, A. C., Shevliakova, E., and Pacala, S. W.: Microbe-driven turnover offsets mineral-
mediated storage of soil carbon under elevated CO₂, *Nature Climate Change*, 4, 1099, <https://doi.org/10.1038/nclimate2436>
<https://www.nature.com/articles/nclimate2436#supplementary-information>, 2014.
- Tang, J. and Riley, W. J.: Competitor and substrate sizes and diffusion together define enzymatic depolymerization and
665 microbial substrate uptake rates, *Soil Biology and Biochemistry*, 139, 107624, <https://doi.org/10.1016/j.soilbio.2019.107624>,
2019.
- Thum, T., Caldararu, S., Engel, J., Kern, M., Pallandt, M., Schnur, R., Yu, L., and Zaehle, S.: A new model of the coupled
carbon, nitrogen, and phosphorus cycles in the terrestrial biosphere (QUINCY v1.0; revision 1996), *Geoscientific Model
Development*, 12, 4781–4802, <https://doi.org/10.5194/gmd-12-4781-2019>, 2019.



- 670 Todd-Brown, K. E. O., Randerson, J. T., Hopkins, F., Arora, V., Hajima, T., Jones, C., Shevliakova, E., Tjiputra, J., Volodin, E., Wu, T., Zhang, Q., and Allison, S. D.: Changes in soil organic carbon storage predicted by Earth system models during the 21st century, *Biogeosciences*, 11, 2341–2356, <https://doi.org/10.5194/bg-11-2341-2014>, 2014.
- Wang, B., An, S., Liang, C., Liu, Y., and Kuzyakov, Y.: Microbial necromass as the source of soil organic carbon in global ecosystems, *Soil Biology and Biochemistry*, 162, 108422, <https://doi.org/10.1016/j.soilbio.2021.108422>, 2021.
- 675 Wang, G., Post, W. M., Mayes, M. A., Frerichs, J. T., and Sindhu, J.: Parameter estimation for models of ligninolytic and cellulolytic enzyme kinetics, *Soil Biology and Biochemistry*, 48, 28–38, <https://doi.org/10.1016/j.soilbio.2012.01.011>, 2012.
- Wang, G., Post, W. M., and Mayes, M. A.: Development of microbial-enzyme-mediated decomposition model parameters through steady-state and dynamic analyses, *Ecological Applications*, 23, 255–272, <https://doi.org/10.1890/12-0681.1>, 2013.
- Wang, G., Huang, W., Zhou, G., Mayes, M. A., and Zhou, J.: Modeling the processes of soil moisture in regulating microbial and carbon-nitrogen cycling, *Journal of Hydrology*, 585, 124777, <https://doi.org/10.1016/j.jhydrol.2020.124777>, 2020.
- 680 Wang, M., Guo, X., Zhang, S., Xiao, L., Mishra, U., Yang, Y., Zhu, B., Wang, G., Mao, X., Qian, T., Jiang, T., Shi, Z., and Luo, Z.: Global soil profiles indicate depth-dependent soil carbon losses under a warmer climate, *Nat Commun*, 13, 5514, <https://doi.org/10.1038/s41467-022-33278-w>, 2022a.
- Wang, Y., Mao, J., Hoffman, F. M., Bonfils, C. J. W., Douville, H., Jin, M., Thornton, P. E., Ricciuto, D. M., Shi, X., Chen, H., Wullschleger, S. D., Piao, S., and Dai, Y.: Quantification of human contribution to soil moisture-based terrestrial aridity, *Nat Commun*, 13, 6848, <https://doi.org/10.1038/s41467-022-34071-5>, 2022b.
- 685 Wickham, H.: *ggplot2*, Springer International Publishing, Cham, <https://doi.org/10.1007/978-3-319-24277-4>, 2016.
- Wickham, H., Averick, M., Bryan, J., Chang, W., McGowan, L., François, R., Golemund, G., Hayes, A., Henry, L., Hester, J., Kuhn, M., Pedersen, T., Miller, E., Bache, S., Müller, K., Ooms, J., Robinson, D., Seidel, D., Spinu, V., Takahashi, K.,
- 690 Vaughan, D., Wilke, C., Woo, K., and Yutani, H.: Welcome to the Tidyverse, *JOSS*, 4, 1686, <https://doi.org/10.21105/joss.01686>, 2019.
- Wieder, W. R., Grandy, A. S., Kallenbach, C. M., and Bonan, G. B.: Integrating microbial physiology and physio-chemical principles in soils with the Microbial-Mineral Carbon Stabilization (MIMICS) model, *Biogeosciences*, 11, 3899–3917, <https://doi.org/10.5194/bg-11-3899-2014>, 2014.
- 695 Wieder, W. R., Allison, S. D., Davidson, E. A., Georgiou, K., Hararuk, O., He, Y., Hopkins, F., Luo, Y., Smith, M. J., Sulman, B., Todd-Brown, K., Wang, Y.-P., Xia, J., and Xu, X.: Explicitly representing soil microbial processes in Earth system models, *Global Biogeochemical Cycles*, 29, 1782–1800, <https://doi.org/10.1002/2015GB005188>, 2015.
- Wieder, W. R., Hartman, M. D., Sulman, B. N., Wang, Y.-P., Koven, C. D., and Bonan, G. B.: Carbon cycle confidence and uncertainty: Exploring variation among soil biogeochemical models, *Global Change Biology*, 24, 1563–1579, <https://doi.org/doi:10.1111/gcb.13979>, 2018.
- 700 Xiao, K.-Q., Zhao, Y., Liang, C., Zhao, M., Moore, O. W., Otero-Fariña, A., Zhu, Y.-G., Johnson, K., and Peacock, C. L.: Introducing the soil mineral carbon pump, *Nat Rev Earth Environ*, 4, 135–136, <https://doi.org/10.1038/s43017-023-00396-y>, 2023.
- Yan, Z., Bond-Lamberty, B., Todd-Brown, K. E., Bailey, V. L., Li, S., Liu, C., and Liu, C.: A moisture function of soil heterotrophic respiration that incorporates microscale processes, *Nature Communications*, 9, 2562, <https://doi.org/10.1038/s41467-018-04971-6>, 2018.
- 705 Yu, L., Ahrens, B., Wutzler, T., Schrumf, M., and Zaehle, S.: Jena Soil Model (JSM v1.0; revision 1934): a microbial soil organic carbon model integrated with nitrogen and phosphorus processes, *Geoscientific Model Development*, 13, 783–803, <https://doi.org/10.5194/gmd-13-783-2020>, 2020.
- 710 Zhang, X., Xie, Z., Ma, Z., Barron-Gafford, G. A., Scott, R. L., and Niu, G.-Y.: A Microbial-Explicit Soil Organic Carbon Decomposition Model (MESDM): Development and Testing at a Semiarid Grassland Site, *Journal of Advances in Modeling Earth Systems*, 14, e2021MS002485, <https://doi.org/10.1029/2021MS002485>, 2022.



Zhang, Z., Pan, Z., Pan, F., Zhang, J., Han, G., Huang, N., Wang, J., Pan, Y., Wang, Z., and Peng, R.: The Change Characteristics and Interactions of Soil Moisture and Temperature in the Farmland in Wuchuan County, Inner Mongolia, China, *Atmosphere*, 11, 503, <https://doi.org/10.3390/atmos11050503>, 2020.